Photolytic and Photocatalytic Destruction of Formaldehyde in Aqueous Media

Eun-Mi Shin, R. Senthurchelvan, J. Munoz, S. Basak, and K. Rajeshwar*

Department of Chemistry and Biochemistry, The University of Texas at Arlington, Arlington, Texas 76019-0065, USA

Gallia Benglas-Smith and Bennett C. Howell, III

Solar Kinetics, Incorporated, Dallas, Texas 75220, USA

ABSTRACT

Formaldehyde (HCHO) was decomposed in UV-irradiated aqueous suspensions of titanium dioxide. Initial HCHO levels in the range 60-1000 ppm, a nominal TiO_2 dose of 1 g/liter, and a medium-pressure Hg lamp were employed in these experiments. Chemical oxygen demand measurements of the solution before and after photocatalytic treatment revealed the mineralization of HCHO to be complete only for the lower end (<100 ppm) of the concentration range. Direct ultraviolet photolysis of HCHO also occurred, but this pathway had an initial lag unlike the photocatalytic route. In the presence of TiO_2 and ultraviolet irradiation, the direct photolysis route was bypassed and the reaction proceeded dominantly by the photocatalytic route. The kinetics of the photocatalytic oxidation of HCHO were analyzed using several models. The effect of H_2O_2 addition to the UV/TiO_2 system was also probed as well as the homogeneous ultraviolet H_2O_2 approach for the treatment of HCHO. The latter exhibited the fastest kinetics for the destruction of HCHO. Finally, the long-term stability and photocatalytic activity of TiO_2 were monitored with two substrates, namely, HCHO and trichloroethylene in two different media: viz. pristine water and a "real-life" water sample with bicarbonate alkalinity. No degradation in the photocatalyst performance was noted over ten repeat use cycles in either case.

Introduction

Much work has been done in recent years on the photocatalytic (PC) treatment of environmental pollutants.[1-4] Heterogeneous photocatalysis involves the use of semiconductor (*e.g.*, TiO_2) suspensions to harness the light and to generate $^{\bullet}OH$ radicals and electrons at the photocatalyst/solution interface. These in turn can be used to destroy and/or immobilize harmful organics/microorganisms and metal ion pollutants, respectively. The PC pollution abatement method can be considered under the umbrella of a number of new technologies, collectively known as advanced oxidation processes, or AOPs.[5] These also include the homogeneous photolysis approach employing either direct ultraviolet (UV) photolysis of the targeted pollutant or the generation of $^{\bullet}OH$ and solvated electrons (e^-_{aq}) by irradiation of H_2O_2, ozone (or combinations thereof), and reagents such as $Fe(CN)_6^{4-}$, [6] respectively. In this paper, we consider the destruction of formaldehyde in water using direct UV photolysis, UV/TiO_2, UV/H_2O_2, and UV/H_2O_2/TiO_2 approaches.

Formaldehyde is considered an irritant,[7] allergen,[8] and a carcinogen.[9] The United States Occupational Safety and Health Administration has recently lowered the permissive exposure limit of this chemical from 1 to 0.75 ppm on an 8 h time-weighted average. The use of formaldehyde in the United States is also regulated via the Federal Insecticide, Fungicide, and Rodenticide Act. It is worth noting that the widespread industrial use of formaldehyde as a resin component, synthetic reagent, tanning agent, disinfectant, bactericide, and preservative has spurred the increasing levels of national production of this chemical (significantly up from the 6,000 lb. level [as 37% solution] in 1976, cf. Ref. 10). The health concerns, however, have prompted the search for alternatives, for *e.g.*, alcohol instead of formalin for tissue fixation applications in the surgical pathology laboratory.[11]

A secondary objective of this study is to address the long-term stability of TiO_2 in PC applications. Given the preponderance of evidence for the adsorption of a variety of organic substrates at the TiO_2 surface (cf. Ref. 12-14), it is of interest to examine whether the PC activity of TiO_2 is adversely affected on long-term contact with organic substrates. In a heterogeneous catalysis context, the adsorption of reactant, intermediate(s), or the product often provokes passivation or fouling of the catalyst surface. It has been reported[15] that TiO_2-coated sand shows no degradation of PC activity over 18 days with salicylic acid as the substrate. When methyl orange was used, however, the PC activity dropped by 28%, and this was attributed to the inhibitory effect of sulfate anion formed as the reaction intermediate.[15] In another study, no degradation of activity was noted over ten repeat use cycles of TiO_2 for the PC treatment of 4-chlorophenol.[16] In the present study, it was decided to use two different media, viz. pristine water and a "real-life" water sample of high bicarbonate alkalinity to test the long-term performance of the TiO_2 photocatalyst. Two different organic substrates, namely, formaldehyde and trichloroethylene (TCE), were also used in the hope that if adsorption did indeed play a role, then this would manifest in different degrees of photocatalyst deactivation, since the reactants, intermediates, and products have distinctly different chemical nature in the two cases. Formic acid is formed as an intermediate in the case of formaldehyde, and chlorinated acetaldehyde and acetic acid derivatives are generated during TiO_2-mediated TCE photodegradation.[17,18] Similarly, CO_2 and H_2O are the mineralization products for formaldehyde, while HCl is additionally formed as an end product in the case of TCE.

Experimental

Chemicals.—All chemicals were ACS reagent grade and were used without further purification except 2,4-pentanedione (acetyl acetone) which was distilled prior to use. All solutions were made up with deionized water (Corning Megapure) unless otherwise noted. Titanium dioxide was from Degussa (P-25) and was predominantly anatase with a specific surface of ~60 m^2/g.

Photoreactor and instrumentation.—The UV photoreactor has been described elsewhere.[19] A 400 W medium pressure Hg lamp (General Electric H400 A 33-1) was used as the UV radiation source. The incident light flux (not corrected for scattering by the suspension or by the reactor wall) was measured by a radiometer/photometer (Biospherical Instruments, San Diego, CA, Model QSL-100). The light intensity was varied from 2.49 to 0.208 $mE/s \cdot m^2$ using neutral density filters as needed.

Analytical details.—The formaldehyde level in solution was assayed by the Nash method.[20,21] The Nash reagent was prepared by mixing 7.5 g of ammonium acetate with 0.1 ml of acetyl acetone. This was dissolved in water to bring the total volume to 25 ml. Then 5 ml of each diluted

* Electrochemical Society Active Member.

sample aliquot from the photoreactor were mixed with 2 ml of the Nash reagent in a test tube and warmed in a water bath at ~60°C for 5 min. The sample was then cooled and transferred to a quartz optical cuvette. The absorbance at 412 nm was measured. Spectrophotometric analyses were performed on a Hewlett-Packard (HP) Model 8452A diode array UV-vis spectrometer fitted with an HP Model 300 desktop computer.

The chemical oxygen demand (COD) of the solutions initially containing formaldehyde was also measured[22] at various intervals of time after the PC treatment. For this, 20 ml of the sample aliquot were mixed with 10 ml of 0.25 *N* $K_2Cr_2O_7$. Then 0.4 g of $HgSO_4$ and boiling chips were added to this solution along with 30 ml of reagent (5.5 g Ag_2SO_4 dissolved in 1 kg of H_2SO_4). The solution was boiled for 2 h, cooled, and the volume made up to 150 ml. A few (3-4) drops of ferroin indicator were added and the solution titrated with 0.25 *N* ferrous ammonium sulfate to a brown color end point. The COD was calculated from the titrimetric data as per the steps outlined in Ref. 22.

The TCE in the solution was determined by gas chromatography (GC) using an HP Model 5890 Series II equipped with a photoionization detector. Sample was introduced in the GC through a Tekmar-7000 head space autosampler. The column used was a Supelco-SPB5 fused silica capillary column (30 m length, 0.53 mm id, and 3.0 μm film thickness). The data were analyzed with an HP 3396 Series II autointegrator. The column temperature program was as follows: 40°C for 4 min, followed by a temperature ramp at 10°C/min to 230°C. A calibration curve was set up with six reference solutions of TCE with concentrations ranging from 0.94 to 14.10 ppm. For the kinetics study, sample aliquots were taken at 0, 5, 10, 15, 20, and 30 min. For long-term TiO_2 stability experiments, samples were taken at 0 and 30 min.

The long-term stability of TiO_2 was also tested in a sample of water supplied by the Kelly Air Force Base, San Antonio, Texas. This sample was spiked with TCE as needed for the PC treatment. This water sample had a pH of 6.78 ± 0.03, zero hydroxide alkalinity, zero carbonate alkalinity, and a bicarbonate alkalinity of 305.5 mg $CaCO_3$/liter as established by titrimetric analyses.[23]

Procedures.—The solutions were sparged with either air, O_2, or N_2 (as needed) for 5 min prior to a PC experiment. During the experiment, ice water was circulated through an annulus surrounding the UV lamp and the top part of the photoreactor. Every precaution was taken in this manner to minimize volatilization (stripping) loss of formaldehyde (or TCE) during a PC reaction run (see below).

For the long-term stability experiments, the solution at the end of a run was spun at 9,000 rpm in a Sorvall Superspeed Model RC 2-B refrigerated centrifuge. The recovered TiO_2 was oven-dried overnight followed by weighing to assess the extent of recovery. Typically, approximately 10% of the catalyst material was inevitably lost after each run. To maintain a constant TiO_2 dose for reuse and also for statistically averaging out run-to-run variations, each run was performed in replicate (3 to 4 times) and the recovered TiO_2 was combined for reuse in a further run. In this manner, up to ten repeat cycles of formaldehyde (or TCE) degradation could be performed with each run. A typical run lasted 3 h in the case of formaldehyde, and 30 min for TCE.

In all the cases, the TiO_2 dose in the solution was 1 g/liter unless otherwise specified. For the UV/H_2O_2 and UV/H_2O_2/TiO_2 experiments, the substrate-to-H_2O_2 mole ratio was maintained at 1:2.

Results and Discussion

Comparison of various photolytic approaches.—Figure 1 contains a comparison of the direct UV photolysis (▲), UV/H_2O_2 (■), UV/TiO_2 (□), and UV/H_2O_2/TiO_2 (O) approaches for the destruction of HCHO in water. A dark control (●) is also included for comparison. The initial concentration of HCHO was maintained constant at 100 ppm for this comparative study. The TiO_2 dose was 1 g/liter, and the H_2O_2 concentration was 226 ppm in all the cases where applicable. Clearly, the UV/H_2O_2 approach outperforms the other AOP candidates tested herein for the treatment of HCHO.

The direct UV photolysis and the UV/TiO_2 routes proceed at essentially similar rates, although careful examination does reveal significant differences in the two cases. Specifically, the direct UV photolysis conversion-time profiles are S-shaped as the replicate analyses in Fig. 2 show. The comparisons contained in Fig. 3a for two different substrate concentrations also show that the direct UV photolysis route lags behind the PC reaction counterpart in the early stages of the reaction. Interestingly, the rate trend switches in the later stages when the direct UV photolysis route becomes more facile than the PC reaction pathway.

These experiments reveal that when TiO_2 particles are also present in the medium, the initial lag disappears. To pursue this theme further, similar experiments were conducted except now the cooling water surrounding the UV lamp was replaced with $CuSO_4$ solution. Copper sulfate

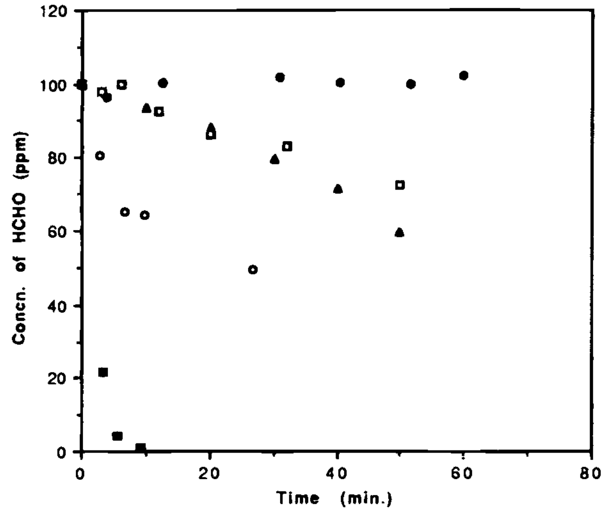

Fig. 1. Comparison of the efficacy of direct UV photolysis (▲), UV/TiO_2 (□), UV/H_2O_2/TiO_2 (O), and UV/H_2O_2 (■) AOPs for the treatment of formaldehyde in water. A dark control experiment (●) is also shown. The initial concentration of formaldehyde was 100 ppm in all the cases. The TiO_2 and H_2O_2 solution doses were 1 g/liter and 226 ppm where applicable. In the dark control case, the solution contained 100 ppm of formaldehyde and 226 ppm of H_2O_2, and was purged with air.

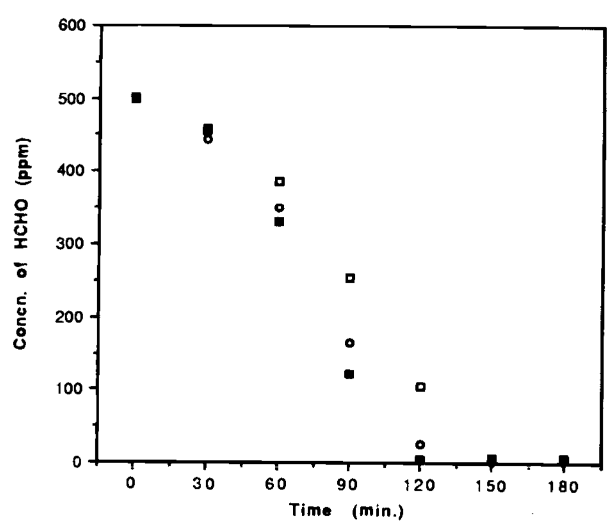

Fig. 2. Three replicate runs for the direct UV photolysis of 500 ppm formaldehyde in water.

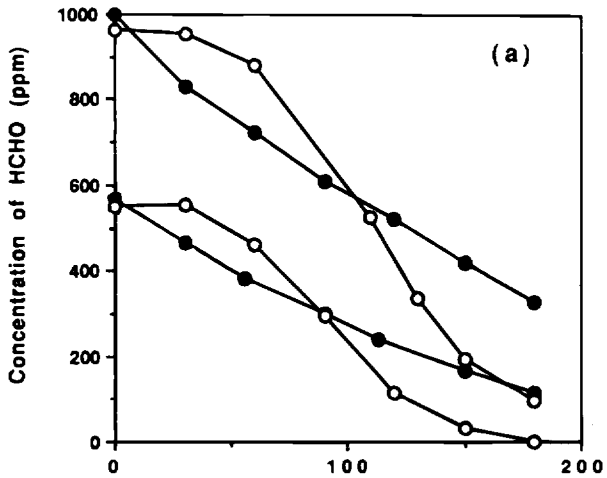

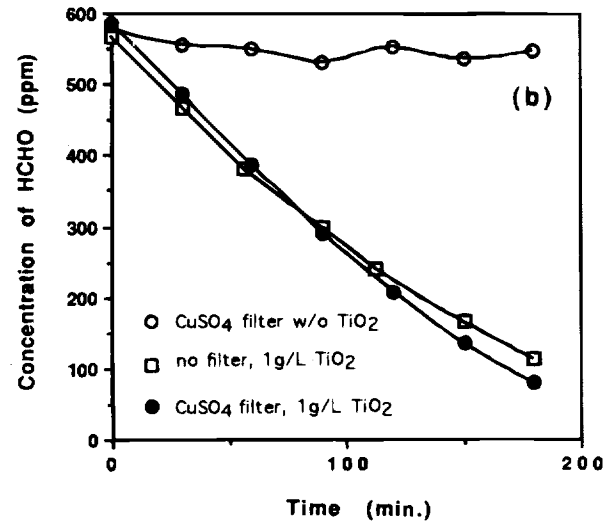

Fig. 3. (a) Plots of concentration of formaldehyde vs. treatment time for two different initial concentrations of formaldehyde (963 and 550 ppm) under different photolysis conditions: O, direct UV photolysis; ●, TiO_2 mediated photolysis. (b) Plot of concentration of formaldehyde vs. treatment time under different photolytic conditions (as specified in the figure).

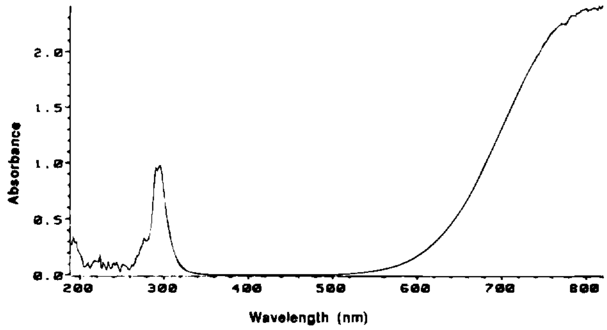

Fig. 4. A UV-Vis spectrum of $CuSO_4$ solution (50 g/liter) in water. Note that the solution absorbs light of wavelengths less than ~350 nm that are important for the direct UV photolysis of organic compounds.

serves as a UV filter to block light below ~300 nm (Fig. 4). In the presence of the $CuSO_4$ filter, the direct photolysis route is precluded as shown by the data in Fig. 3b. Interestingly, the shape of the conversion curve reverts to the one observed with TiO_2 in the absence of the short wavelength filter. The results in Fig. 3b appear to support rather conclusively the notion that the PC reaction route supercedes the direct UV photolysis route when TiO_2 is also present in the medium.

The medium pH (which was not controlled) in both cases progressively became more acidic as the reaction proceeded. After about 1 h, the pH reverted slowly back to the starting value. A reasonable explanation is that formic acid is generated as an intermediate. As this intermediate is then further oxidized to CO_2, the pH begins to rise. Table I contains the results from COD analyses of a range of HCHO-containing solutions that were subjected to the PC oxidation treatment. Negligible levels of COD are attained only for the lowest substrate level (100 ppm) considered herein. In all the other cases, the mineralization is incomplete even after ~3 h.

The last two sets of columns in Table I compare the COD test results with the carbon content of the solution as calculated from the formaldehyde analyses. The discrepancy between the two sets of "before" values can be rationalized on the basis of the presence of other carbonaceous compounds in the starting solution (*e.g.*, methanol that is added as a stabilizer) that are not detected by the Nash method. For example, the formaldehyde sample as supplied by the manufacturer is quoted to contain 10-15% CH_3OH and 37 weight percent of HCHO. This would translate to a carbon content (from methanol) of ~93.6 ppm. The combined carbon content registered by the Nash method (398 ppm) and this value amounts to 491.6 ppm, which is in good agreement with that measured in the COD test (Table I). Similarly, the "after" values are at variance because of the presence of reaction intermediate(s), *e.g.*, formic acid, that are also not detected by the Nash method.

The lag in the PC conversion route in the later stages (cf. Fig. 1 and 3a) is probably a consequence of O_2 starvation. This is a serious handicap with the UV/TiO_2 method. Consider the reaction

$$HCHO + O_2 \xrightarrow[TiO_2]{h\nu} CO_2 + H_2O \quad [1]$$

For a 1000 ppm load of the substrate, the stoichiometric O_2 amount needed would be 0.033 *M*. However, the nominal O_2 solubility in aqueous media is only 0.0012 *M*.[24] This level of O_2 availability would be inadequate even for an initial HCHO concentration of 100 ppm. This is certainly reflected in the data in Fig. 1.

Table I. Chemical oxygen demand and residual carbon content of solution before and after PC treatment with UV-irradiated TiO_2.[a]

Initial HCHO concentration (ppm)	COD values (ppm)		Carbon content (ppm) From COD		Carbon content (ppm) From Nash test	
	Before	After	Before	After	Before	After
1000	1324	648	496	256	398	131
700	1305	139	489	52	274	42
500	1089	133	409	50	235	32
300	533	124	200	46	137	32
100	189	6	71	2	44	0

[a] Photocatalytic treatment for 3 h.

The dramatic improvement in the PC oxidation rate on H_2O_2 addition (Fig. 1) is not unexpected, and similar observations have been made by previous authors for other substrates.[1-3] The beneficial effects of H_2O_2 in a UV/TiO_2 system are twofold: (*i*) H_2O_2 generates additional $^{\bullet}OH$ via photolysis.[25] (*ii*) H_2O_2 is a facile electron acceptor and thus improves the quantum yield for the photoassisted reactions at the TiO_2/water interface.

Influence of purge gas and light intensity on formaldehyde PC degradation.—As discussed elsewhere,[1-4,19] the nature of the purge gas influences the PC oxidation rate through the electron transfer reaction

$$O_2 + e^- \rightarrow O_2^- \text{ etc.} \qquad [2]$$

When this purge reaction is progressively "shut down" with replacement of the O_2-saturated solution with air and N_2 in turn, the PC (hole) reaction also suffers because of the accumulation of electrons and the consequent increase in the e^--h^+ recombination rate. This is illustrated in Fig. 5. We have seen a similar effect earlier on the ability of UV-irradiated TiO_2 to kill bacteria (*E. coli*).[26] On the other hand, when the PC process of interest involved the reduction of Cr(VI) to Cr(III) at TiO_2, the presence of O_2 had a deleterious effect because of the resulting competition between the two oxidants for the photogenerated electrons.[19]

It is noteworthy that the conversion of formaldehyde is not completely "shut down" in the presence of N_2 purge (Fig. 5). Traces of (electron acceptor) impurities or adventitious O_2 in the solution can explain this observation. Blank runs with air flow in the dark show that loss of HCHO by stripping is significant only at times longer than ~180 min.

If the quantum yield, ϕ, is independent of the incident light flux (I_L), the PC degradation rate will be a linear function of the latter.[27] On the other hand, either high light fluxes and/or rather sluggish reaction kinetics at the TiO_2 particle-solution boundary will result in the interfacial accumulation of the photogenerated e^--h^+ pairs and consequent pair recombination. The result is a decrease in ϕ with increasing I_L. Indeed, transitions have been observed in regimes of rate (or ϕ) *vs.* I_L behavior progressing from linear (constant) through $I_L^{0.5}$ ($I_L^{-0.5}$) to I_L indepedent (I_L^{-1}).[28]

Figure 6 contains data from this study addressing the issue of the light flux dependence of the PC oxidation of formaldehyde. Figure 6a contains conversion-time plots with I_L as the parameter for an initial formaldehyde concentration of ~ 60 ppm. A log-log plot of the initial rate (R) *vs.* I_L (Fig. 6b) yields an exponent of ~0.43. That is, an approximately square-root dependence is observed,[29] signifying that e^--h^+ pair recombination competes significantly with interfacial charge-transfer under the conditions pertinent to our experiments.

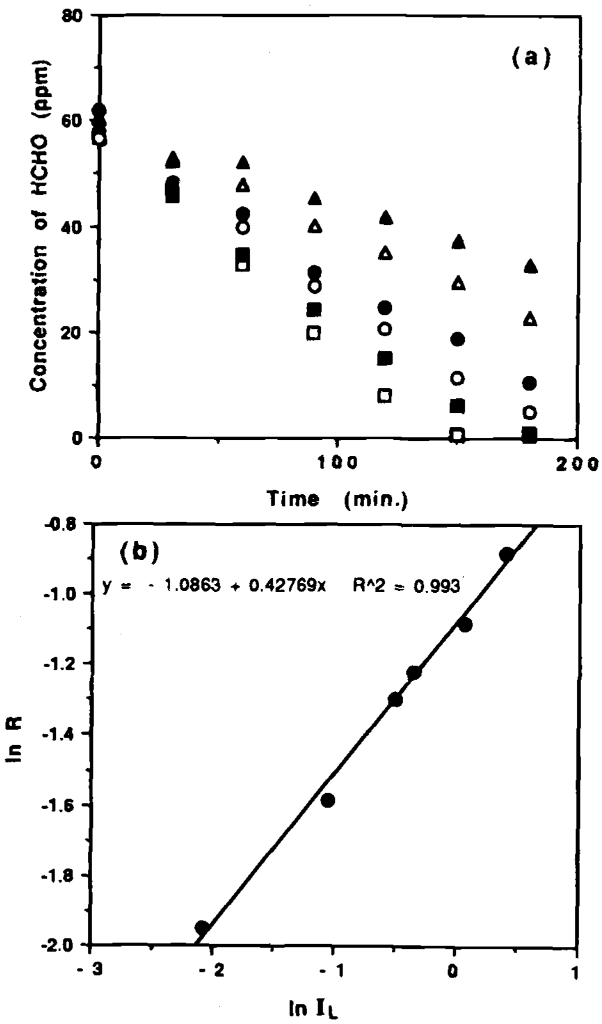

Fig. 6. (a) Plots of concentration of formaldehyde *vs.* PC treatment time for different light intensities (μE/s · cm²): □ – 0.249; ■ – 0.177, ○ – 0.116, ● – 0.101, △ – 0.058, and ▲ – 0.021. (b) A ln-ln plot of the initial PC reaction rate (R) *vs.* light intensity (I_L).

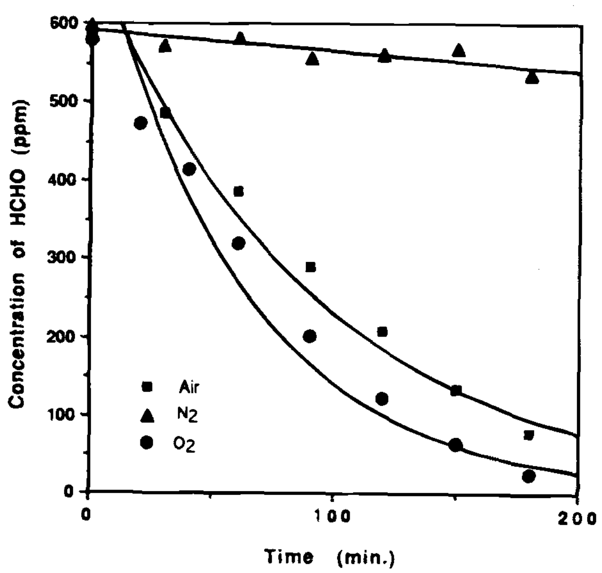

Fig. 5. Plots of concentration of formaldehyde *vs.* PC treatment time in various gaseous ambients (as specified in the figure).

Photocatalysis kinetics for formaldehyde.—The kinetics of the UV/H_2O_2 and UV/TiO_2 reactions were analyzed in detail for formaldehyde as the substrate. Figure 7a illustrates the variation of formaldehyde concentration in solution with time for five different initial levels ranging from 100 to 1,000 ppm. The percent conversion *vs.* time data for these experiments are contained in Fig. 7b. For the lowest initial concentration (100 ppm), 100% conversion is attained at ~50 min under these conditions.

Photocatalysis kinetics data have been analyzed using the Langmuir-Hinshelwood (L-H) model[1-3] expressed in the form

$$R = \frac{k'\kappa c_o}{1 + \kappa c_o} \qquad [3]$$

In Eq. 3, R is the intial PC rate, c_o is the initial substrate concentration, k' is the saturation rate (see below), and κ is an equilibrium constant describing substrate-TiO_2 interactions. Figure 8a contains a plot of the initial PC rate *vs.* the formaldehyde concentration. The initial rate was obtained from the slope of the percent conversion *vs.* time curves (cf. Fig. 7b). The sharp (linear) rise in the rate at low levels of the substrate followed by a tendency toward rate saturation is typical of L-H kinetics behavior. A re-expression of Eq. 3 in the inverse form[17,30]

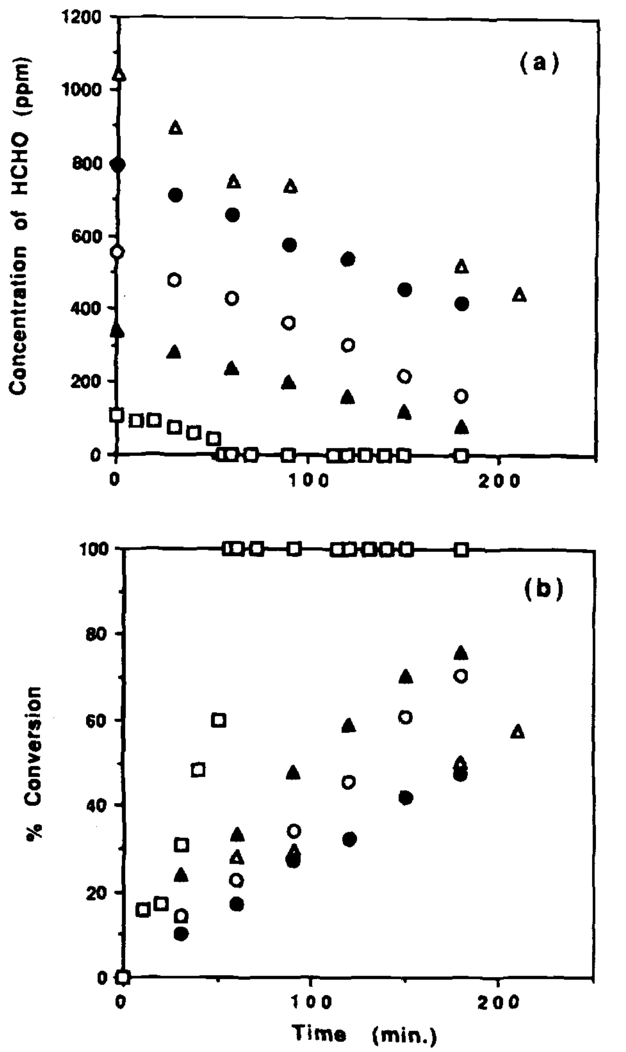

Fig. 7. (a) Plots of concentration of formaldehyde *vs.* treatment time with initial concentrations of formaldehyde as a parameter: △ – 1044 ppm; ● – 792 ppm; ○ – 555 ppm; ▲ – 349 ppm; and □ – 111 ppm. (b) Plots of percent conversion of formaldehyde *vs.* treatment time from these data. The symbols are as in (a). The photocatalytic treatment conditions are specified in the Experimental section.

$$1/R = 1/k' + (1/k'\kappa)\cdot(1/c_o) \quad [4]$$

affords a route to determination of k' and κ from a plot of $1/R$ *vs.* $1/c_o$ (Fig. 8b). Values for the L-H kinetics parameters of 3.11 ppm min^{-1} and 4.22×10^{-3} ppm^{-1} were obtained for k' and κ, respectively, from the least squares fits in Fig. 8a and b.

The rate parameter, k' in the L-H model expression (Eq. 3 and 4) is generally interpreted[1-3] in terms of reflecting the limiting rate at high solute concentrations, *i.e.*, when $\kappa c_o >> 1$

$$R \simeq k' \quad [5]$$

In this situation, essentially all the TiO_2 surface sites available for adsorbing the substrate are occupied. On the other hand, the parameter κ reflects the ability fo the substrate to be "bound" or adsorbed at the TiO_2 surface. However, it has been noted[1-3,28,30] that these parameters have only procedural (rather than molecular) significance.

The initial rate *vs.* concentration data can also be analyzed in a general manner starting with the expression

$$R = kc_o^n \quad [6]$$

In Eq. 6, k is the rate constant and n is the reaction order. Thus, a ln-ln plot of the rate *vs.* the initial concentration

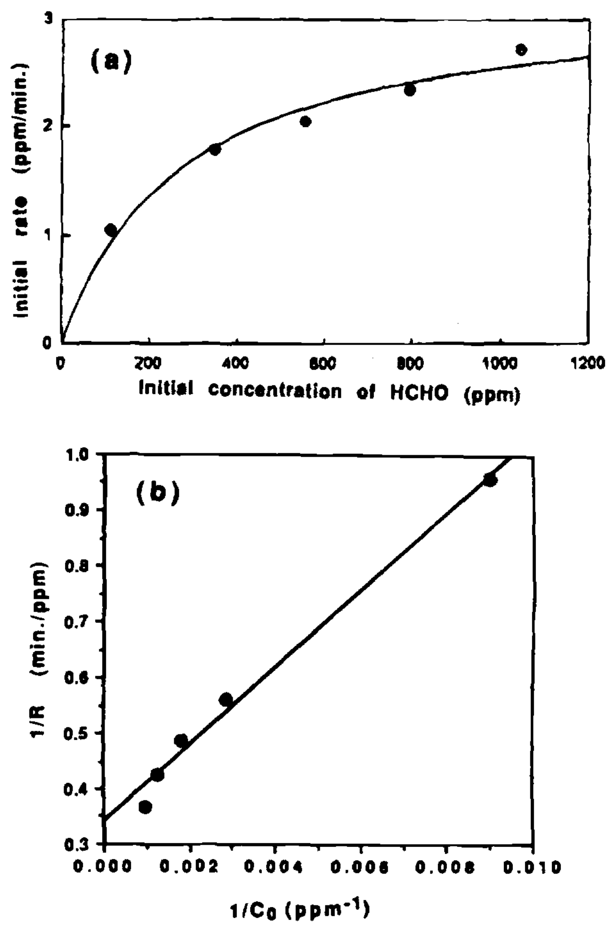

Fig. 8. (a) Plot of initial PC reaction rate *vs.* the initial concentration of formaldehyde. The solid line is a nonlinear least squares fit and the dots represent the experimental data. (b) The corresponding plot of the inverse rate ($1/R$) *vs.* the inverse initial concentration of formaldehyde ($1/c_o$) (cf. Eq. 4).

(Fig. 9a) affords a route to k and n. Values of 0.15 and 0.42 were obtained for the two parameters, respectively.

Starting with Eq. 6, a method of kinetics analysis based on continuous monitoring of the reaction half-life, $t_{1/2}$, as a function of time can be used.[31] It can be shown (cf. Appendix) that

$$\log t_{1/2} = \log\left[\frac{(2^{n-1} - 1)}{k(n - 1)}\right] + (1 - n)\log c_o \quad [7]$$

The advantage of this method of kinetics analysis is that a plot of log $t_{1/2}$ *vs.* log c_o enables computation of k and n from a single experiment. In other words, c_o is employed as a running variable. For example, if c_o = 300 ppm, the time required for the concentration to change from 300 to 150 ppm, 290 to 145 ppm, 280 to 140 ppm, etc., can be continually mapped. Figure 9b contains a representative plot of Eq. 7 for one set of formaldehyde conversion data from this study. Values for k and n of 0.28 and 0.37 were obtained in reasonable agreement with the analyses from Fig. 9a.

Obviously, the method based on Eq. 7 cannot be used for the analysis of first-order kinetics cases wherein $t_{1/2}$ will be constant (and independent of c_o). An example of this will be encountered for the TCE case presented later. We suggest that a plot of $t_{1/2}$ *vs.* c_o be first made to verify that the system indeed is not first order. We are not aware of previous instances where PC reaction kinetics have been analyzed via the half-life method based on Eq. 7. Again, the important practical advantage of this methodology is

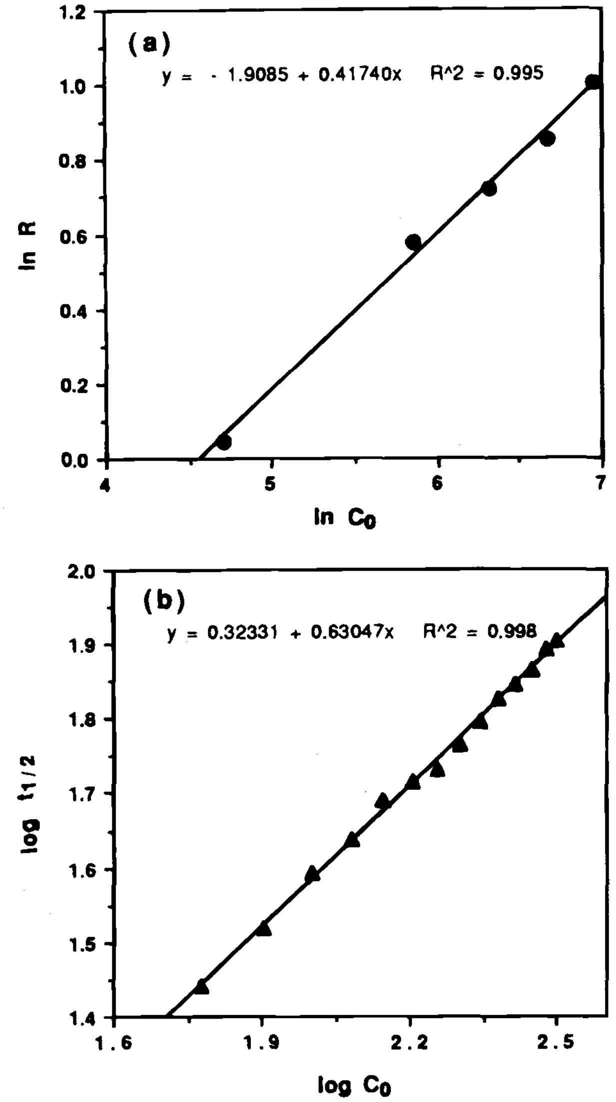

Fig. 9. (a) A ln-ln plot of the PC reaction rate (R) vs. the initial concentration of formaldehyde (c_o). (b) A log-log plot of $t_{1/2}$ (the half-life) vs. the initial concentration of formaldehyde (c_o).

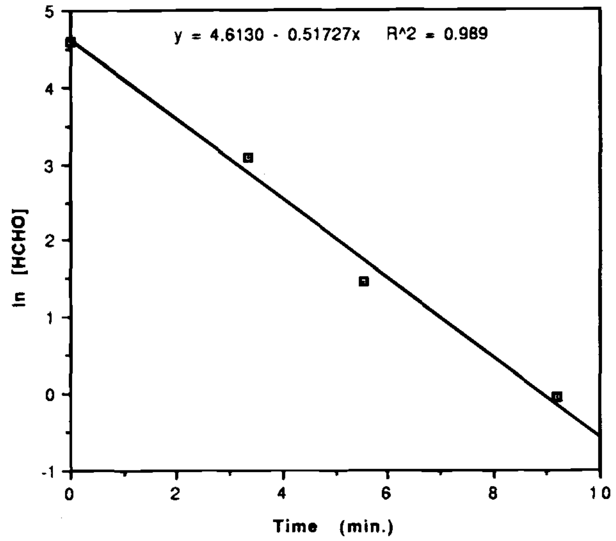

Fig. 10. First-order kinetics plot for the UV/H_2O_2 photolysis of formaldehyde. Data from Fig. 1. The line is a least squares fit with the parameters shown on the figure.

that only a single run is needed, and the analysis is much less tedious than that based on variation of c_o in separate experiments (cf. Fig. 9a).

Fractional reaction orders are not uncommon in heterogeneous reaction kinetics (for example Ref. 32). They are symptomatic of the importance of surface (adsorption) phenomena. The adsorption equilibrium constant, κ, discussed earlier, becomes progressively important as the substrate concentration is decreased. Thus, a substrate recognized as being difficult to oxidize at high concentrations may be oxidized comparatively rapidly at low levels because of its strong interaction with the TiO_2 surface. Formaldehyde certainly appears to belong to this category.

The UV/H_2O_2 conversion data in Fig. 1 fit first-order (or more correctly, pseudo-first-order) reaction kinetics as the analysis in Fig. 10 shows. A rate constant of 0.52 min^{-1} is obtained from the slope of the semilogarithimic plot in Fig. 10. Unfortunately, this rate constant cannot be compared with that determined for the UV/TiO_2 case (because of the variant reaction order in the two cases). However, this rate constant even exceeds that obtained for TCE, a substrate that is considered to be eminently suited to the application of AOPs.

PC degradation of TCE at UV-irradiated TiO_2 suspension.—A brief examination of the PC oxidation kinetics was undertaken for TCE as a prelude to the long-term TiO_2 stability experiments discussed in the next section. As mentioned earlier, the Kelly Air Force Base water sample was used for this phase of the study. Another objective of this portion of the study was to illustrate the contrast in the decomposition kinetics for formaldehyde and TCE as revealed by the usual first-order kinetics analysis and our $t_{1/2}$-based protocol. Specifically, under conditions wherein $\kappa c_o << 1$, Eq. 3 collapses to the first-order expression of Eq. 8

$$R \simeq k' \kappa c_o \equiv k'' c_o \quad [8]$$

Alternatively stated, a plot of of ln c *vs.* time should be linear for first-order kinetics as revealed by integration of Eq. 8 (cf. Fig. 10). This is indeed obeyed for TCE, as shown in Fig. 11b which was generated from the conversion data in Fig. 11a. Equivalently, a plot of log $t_{1/2}$ *vs.* log c_o (cf. Eq. 7) is horizontal (Fig. 11c), supporting the veracity of our kinetics analyses based on the computation of $t_{1/2}$ from a single run.

Representative GC traces from which the data in Fig. 11 were obtained are contained in Fig. 12.

Long-term stability of TiO_2 in the PC oxidation of formaldehyde and TCE.—The TiO_2 photocatalyst was reused over ten repeat cycles as described in the Experimental section. The percent conversion after a fixed time (180 min for formaldehyde and 30 min for TCE) stayed consistently above ~92% for formaldehyde and even higher (above ~98%) for TCE, as detailed in Table II. The relative constancy of k'' and n in the case of formaldehyde (Table II) also supports the absence of significant degradation in the performance of the photocatalyst. Importantly, no pattern was observed in these parameters and also in the extent of conversion over the ten reuse cycles.

Conclusion

Several conclusions emerge from this study:

1. Of the AOPs included in this study, viz. direct UV photolysis, UV/TiO_2, and UV/H_2O_2, UV/H_2O_2 afforded the fastest destruction of formaldehyde. Even the addition of H_2O_2 to the UV/TiO_2 system did not bring the latter on par with UV/H_2O_2, although it did result in rather dramatic improvement relative to the situation in the absence of H_2O_2 in the TiO_2 suspension. The UV/H_2O_2 system showed first-order reaction kinetics with an associated rate constant even exceeding that in the model TCE case.

2. A comparison of the TiO_2-based PC reaction route and direct UV photolysis shows an initial lag for conversion of formaldehyde in the latter case. At later stages, however,

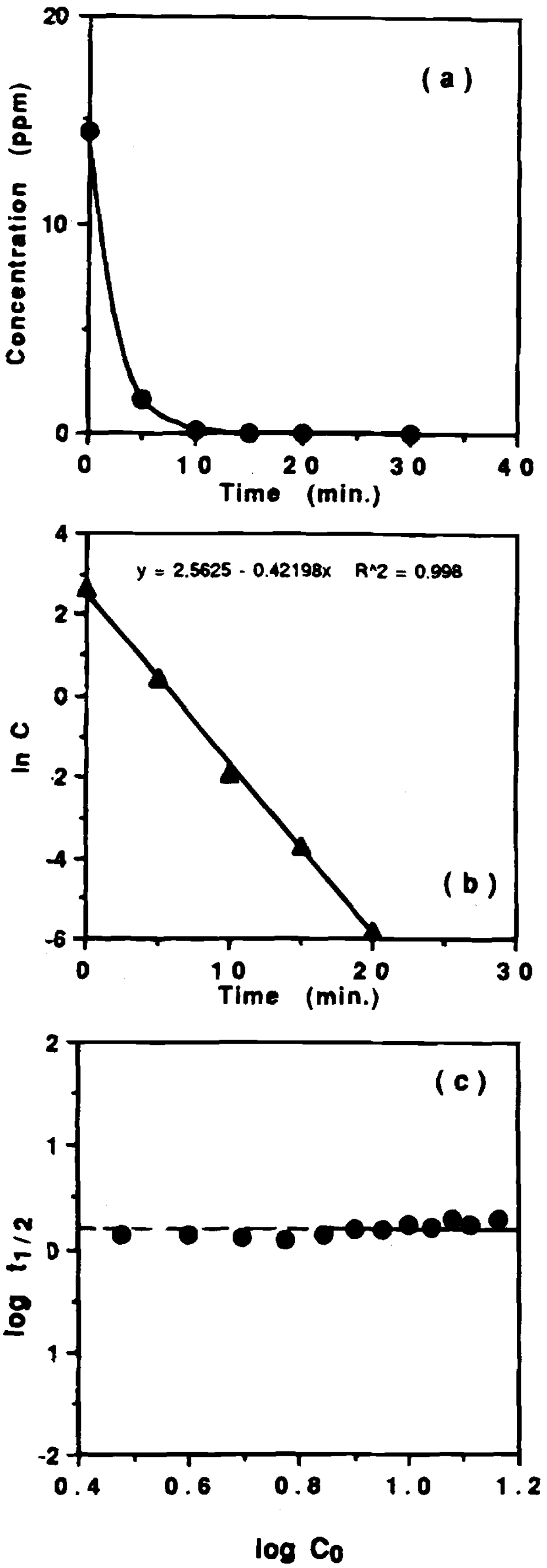

Fig. 11. (a) Variation of trichloroethylene concentration *vs.* PC treatment time for Kelly Air Force Base water. (b) ln *c* (concentration) vs. time plot of the data in (a). (c) A log-log plot of $t_{1/2}$ (half-life) *vs.* concentration of trichloroethylene (c_o).

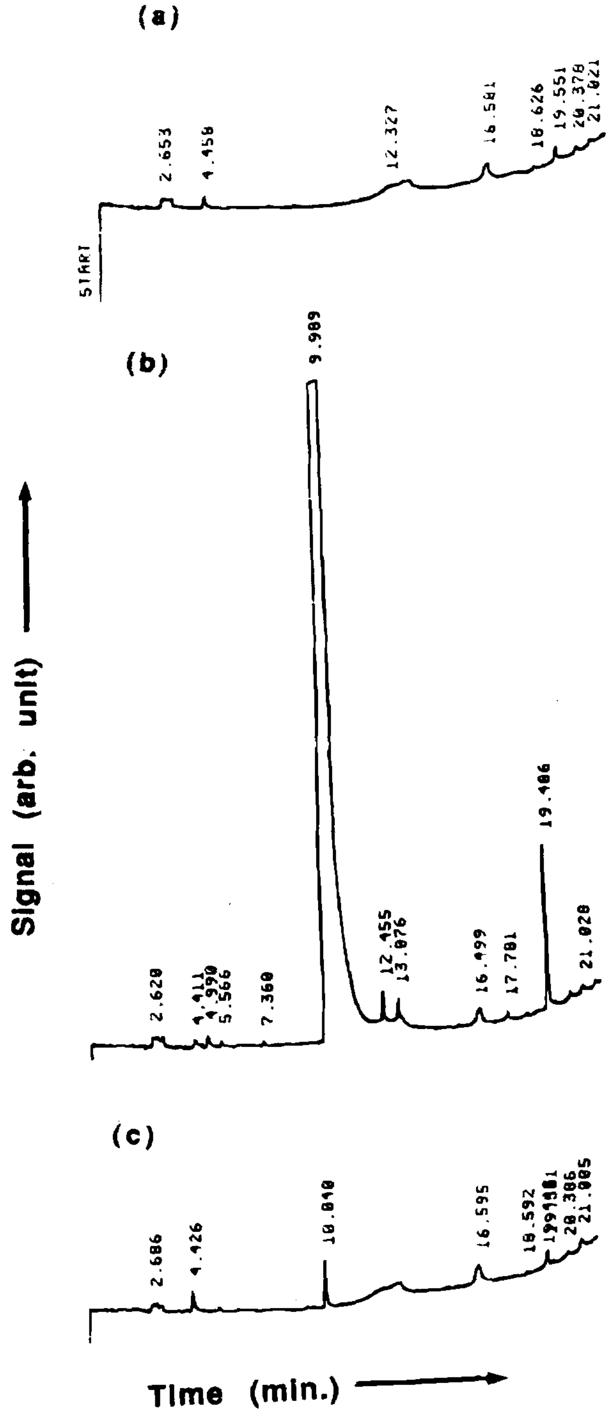

Fig. 12. Gas chromatograms of various solutions: (a) Kelly Air Force Base water; (b) Kelly Air Force Base water spiked with ~15 ppm trichloroethylene; (c) after TiO_2-mediated PC degradation of solution (b). Photocatalysis conditions are specified in the text.

the direct UV photolysis route is faster than the UV/TiO_2 case, probably because of O_2 starvation and reaction intermediate accumulation. Analyses of the COD of various solutions are consistent with this notion.

3. No degradation in the performance of the photocatalyst occurs for at least ten repeat use cycles even at rather high initial levels of pollutant (~300 ppm for formaldehyde) and in "real-life" water medium containing bicarbonate (and possibly a variety of other anions).

4. The kinetics analysis protocol based on $t_{1/2}$ analyses from a single run is effective for a quick diagnosis of the reaction order and the rate parameter. This method can serve as a prelude to more detailed analyses based on the Langmuir-Hinshelwood model and experiments wherein the initial substrate concentration is systematically varied.

Table II. Long-term stability of TiO_2 photocatalyst after formaldehyde and TCE treatment.[a]

Formaldehyde			
Cycle no.	k	n	Percent conversion
1	0.27[b]	0.37[b]	92.9
5	0.35	0.35	98.6
8	0.28	0.36	93.9
9	0.30	0.36	98.6
10	0.27	0.39	98.5
TCE			
Cycle no.	Percent conversion	Cycle no.	Percent conversion
1	99.9	6	99.4
2	99.6	7	98.2
3	99.7	8	99.9
4	98.9	9	99.9
5	99.1	10	99.9

[a] PC treatment times were 180 min and 30 min for HCHO and TCE, respectively (see text). The initial levels of substrate in each cycle were ~300 and ~15 ppm. Pristine water was used for formaldehyde and the Kelly Air Force Base water for TCE.
[b] Data from Fig. 7b.

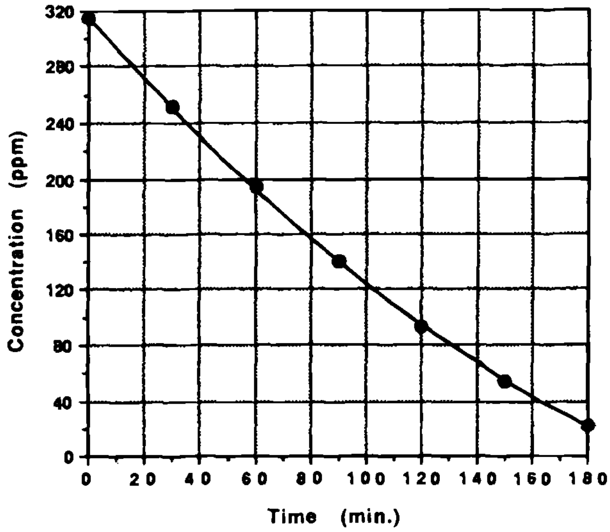

Fig. 1-A. Representative plot of concentration of formaldehyde vs. PC treatment time.

Acknowledgments

This research was supported, in part, by funds from the National Renewable Energy Institute (NREL) under Contract ZAE-3-12314-03. The participation of J. M. in the project at U. T. Arlington in summer, 1994, was enabled by the support of the National Science Foundation, Alliance for Minority Participation Program. We also thank Ed Wolfrum of NREL and David White of Solar Kinetics, Inc., for their interest and support of this research; Martin Pomerantz for loan of the photoreactor; Rohini C. Krishnan, M.D., for discussions on the hazards associated with the use of formaldehyde in the surgical pathology laboratory; Wesley Wampler for providing the nonlinear least squares fitting software (cf. Fig. 8a); and Gloria Madden for assistance in the preparation of this manuscript.

Manuscript submitted Sept. 11, 1995; revised manuscript received Jan. 31, 1996.

Solar Kinetics, Incorporated, assisted in meeting the publication costs of this article.

APPENDIX

We present a method for kinetics analysis[31] based on continuous monitoring of the reaction half-life, $t_{1/2}$, as a function of time. The idea is that in data such as those in Fig. 1-A, the "initial" concentration of the substrate is continually changing, and thus the time required for the concentration to drop to one-half (or any other characteristic fraction) of its initial value can be continuously monitored. Consider the general rate expression

$$\text{rate} = k[c]^n$$

$$-\frac{d[c]}{dt} = k[c]^n$$

$$\frac{d[c]}{[c]^n} = -kdt$$

In the above equations, k is the rate constant, c is the substrate concentration, and n is the reaction order. Integrating the above expression

$$\int_{c_o}^{c_t} \frac{d[c]}{[c]^n} = -\int_0^t kdt$$

$$\frac{[c]^{-n+1}}{-n+1}\Big]_{c_o}^{c_t} = -kt\Big]_0^t$$

or

$$\frac{[c_t]^{-n+1} - [c_o]^{-n+1}}{-n+1} = -k(t - t_0)$$

$$\therefore [c_t]^{-n+1} - [c_o]^{-n+1} = k(n-1)(t - t_0)$$

or

$$\left[\frac{c_t}{c_o}\right]^{-n+1} - 1 = \frac{k(n-1)(t-t_0)}{[c_o]^{-n+1}}$$

In the above equations, c_o is the "initial" concentration, c_t is the concentration at any time, t and t_0 are the "initial" time. When $c_t/c_o = 1/2$, $(t - t_0)$ becomes $t_{1/2}$, the reaction half-life

Therefore

$$(1/2)^{-n+1} - 1 = \frac{k(n-1)t_{1/2}}{[c_o]^{-n+1}}$$

or

$$(2^{n-1} - 1) = \frac{k(n-1)t_{1/2}}{[c_o]^{-n+1}}$$

Therefore

$$t_{1/2} = \frac{(2^{n-1} - 1)\cdot[c_o]^{-n+1}}{k(n-1)}$$

Therefore

$$\log t_{1/2} = \log\left[\frac{(2^{n-1} - 1)}{k(n-1)}\right] + (1-n)\log c_o$$

Thus, a plot of $\log t_{1/2}$ *vs.* $\log c_o$ enables computation of k and n from a single experiment (cf. Fig. 9b in the text).

The above analysis obviously is not applicable to a first-order reaction for which $t_{1/2}$ is constant. This is exemplified by Fig. 11c in the text.

REFERENCES

1. K. Rajeshwar, *J. Appl. Electrochem.*, **25**, 1067 (1995).
2. K. Rajeshwar and J. G. Ibanez, *Environmental Electrochemistry*, Academic Press, San Diego, CA, In press.
3. *Proc. 1st International Conference on TiO_2 Photocatalytic Purification and Treatment of Water and Air*, D. F. Ollis and H. Al-Ekabi, Editors, Elsevier, Amsterdam (1993).
4. K. Rajeshwar and J. G. Ibanez, *J. Chem. Educ.*, **72**, 1044 (1995).
5. W. W. Eckenfelder, A. R. Bowers, and J. A. Roth, Editors, *Chemical Oxidation Technologies for the Nineties*, Vol. 3, Technomic Publishing, Lancaster and Basel (1993).
6. J. R. Bolton and S. R. Cater, in *Aquatic and Surface Photochemistry*, G. R. Helz, R. G. Zepp, and D. G. Crosby, Editors, Lewis Publishers, Boca Raton, FL (1994).
7. J. Bousquet and F-B. Michel, *Clin. Rev. Allergy*, **9**, 357 (1991).
8. E. Cronin, *Contact Dermatitis*, **25**, 276 (1991).
9. T. L. Vaughan, *et al.*, *Int. J. Cancer*, **38**, 685 (1986).

10. J. F. Walker, in *Formaldehyde*, ACS Monograph 159, 3rd ed., p. 552, Krieger, New York (1975).
11. D. G. Bostwick, *Arch. Pathol. Lab. Med.*, **118**, 298 (1994).
12. S. Tunesi and M. Anderson, *J. Phys. Chem.*, **95**, 3399 (1991).
13. J. Cunningham and P. Sedlak, in Ref. 3, p. 67.
14. J. Cunningham and G. Al-Sayyed, *J. Chem. Soc., Faraday Trans.*, **86**, 3935 (1990).
15. R. W. Matthews, *Water Res.*, **25**, 1169 (1991).
16. G. Al-Sayyed, J-C. D'Oliveira, and P. Pichat, *J. Photochem. Photobiol. A*, **58**, 99 (1991).
17. A. L. Pruden and D. F. Ollis, *J. Catal.*, **82**, 404 (1983).
18. W. H. Glaze, J. F. Kenneke, and J. L. Ferry, *Environ. Sci. Technol.*, **27**, 177 (1993).
19. W-Y. Lin, C. Wei, and K. Rajeshwar, *This Journal*, **140**, 2477 (1993).
20. T. Nash, *Biochem.*, **53**, 41 (1953).
21. R. V. Smith and P. W. Erhardt, *Anal. Chem.*, **47**, 246 (1975).
22. *Water and Wastewater Analysis*, American Public Health Association, Washington, DC (1992).
23. *Water and Wastewater Examination Manual*, p. 168, Lewis Publishers, Boca Raton, FL (1990).
24. *CRC Handbook of Chemistry and Physics*, Section 6-4, 73rd ed., CRC Press, Boca Raton, FL (1992-93).
25. S. Lunak and P. Sedlak, *J. Photochem. Photobiol. A*, **68**, 1 (1992).
26. C. Wei, Z. Zainal, W-Y. Lin, N. Williams, R. L. Smith, K. Rajeshwar, and A. Kruzic, *Environ. Sci. Technol.*, **28**, 934 (1994).
27. For example, C. Kormann, D. W. Bahnemann, and M. R. Hoffman, *ibid.*, **25**, 494 (1991).
28. D. F. Ollis, E. Pelizzetti, and N. Serpone, *ibid.*, **25**, 1523 (1991).
29. T. A. Egerton and C. J. King, *J. Oil Colour Chem. Assoc.*, **62**, 386 (1979).
30. D. F. Ollis, *Environ. Sci. Technol.*, **19**, 480 (1985).
31. I. N. Levine, *Physical Chemistry*, 3rd ed., McGraw-Hill, New York (1988).
32. For example, W. E. Garner, *Chemistry of the Solid State*, Butterworths, London (1955).

Studies of Niobium Electrocrystallization Phenomena in Molten Fluorides

P. Chamelot, B. Lafage, and P. Taxil

Laboratoire de Génie Chimique et Electrochimie, URA CNRS 192, Université Paul-Sabatier, 31062 Toulouse Cedex, France

ABSTRACT

The electrodeposition of niobium from $NbCl_5$ or K_2NbF_7, dissolved in molten alkaline fluorides (LiF/NaF), in the 700-800°C temperature range has been studied by using cyclic voltammetry, chronopotentiometry, and chronoamperometry. A linear relationship between the Nb^{IV} diffusion coefficient and the temperature was found in the cyclic voltammograms and chronopotentiograms. Scanning electron micrography shows that the shape of the nuclei is hemispherical. Chronoamperometric results show that the deposition process involves instantaneous nucleation with diffusion-controlled growth of the nuclei. The influence of temperature, overpotential, and substrate (copper, stainless steel, vitreaus carbon) on the nuclear site densities is also considered.

Introduction

An increasing number of applications are being found for niobium in high-technology areas such as nuclear power, space, or microelectronics due to its properties. Niobium is a refractory metal with a melting point of 2465°C,[1] having superconducting properties on its own or when alloyed with other metals such as germanium, zirconium, vanadium, or tin.[2,3] It is resistant to humid corrosion in a highly acid environment subsequent to the formation of a particularly stable passivating surface layer of niobium oxide.[24] However, niobium is not frequently used due to its high cost and the inevitable presence of a large amount of impurities when it is prepared using thermometallugical methods.[1,5] Therefore, niobium production is being considered by means of an electrolysis process in a molten salts electrolyte, which would make it possible to lower the temperature at which the metal is obtained while improving its purity.[6] Furthermore, the applications of this metal related to its surface properties are facilitated by using it in thin-layer form on an ordinary substrate, due to its high price. The thin-layer deposit can be made by electrolysis in molten salts.

The first coherent and adhesive deposits were obtained in the sixties by Senderoff and Mellors.[7] The electrolyte consisted of an LiF/NaF/KF eutectic mixture as solvent and K_2NbF_7 as solute heated to approximately 800°C. These authors proposed a three-stage mechanism leading to the deposit of the niobium, which is now vigorously challenged.[8-10]

In a first article devoted to the reduction of niobium ions in the eutectic LiF/NaF, we proposed another mechanism comprised of the following two stages[11]

$$Nb^{V} + 1e^- \leftrightharpoons Nb^{IV}$$

$$Nb^{IV} + 4e^- \leftrightharpoons Nb$$

This mechanism has been approved by Christensen *et al.*[8]

In agreement with all the authors who have worked on this subject, we also insisted on the need to eliminate beforehand the Nb^{V} ions, which would be liable to oxidize the niobium deposits as soon as they were formed as Nb^{IV} ions.[7,12-15] The purpose of this work is to complete the works presented in the previous article[11] with detailed studies of the nucleation of niobium in molten fluorides. First we checked the results acquired by cyclic voltammetry and chronopotentiometry, while making every effort to acquire additional information that would subsequently be of use on the electrochemical system involved, in particular by calculating the diffusion coefficient of the Nb^{IV} ion at different temperatures. The niobium nucleation phenomenon and the initial growth of the crystals were then studied by chronoamperometry. The goal was to obtain information on the phenomena involved in the initial phase of deposit electrolysis in order to optimize a strategy for making niobium coatings.

Experimental

The cell.—The cell consists of a vitreous carbon crucible (Carbone Lorraine, V25 quality) placed in a cylindrical vessel made of refractory steel and closed by a stainless steel lid cooled by circulating water. Sealing is ensured by Viton O-rings. The inside of the walls are protected against salt vapors by graphite liner. The setup is shown in Fig. 1. The electrodes are attached to the end of nickel rods